# Reactive Oxygen Species and Extracellular Signal-Regulated Kinase 1/2 Mediate Hexachlorobenzene-Induced Cell Death in FRTL-5 Rat Thyroid Cells

Florencia Chiappini, Carolina Pontillo, Andrea S. Randi, Laura Alvarez, and Diana L. Kleiman de Pisarev[1]

*Departamento de Bioquímica Humana, Facultad de Medicina, Universidad de Buenos Aires, 1121 Buenos Aires, Argentina*

[1]To whom correspondence should be addressed at Departamento de Bioquímica Humana, Facultad de Medicina, Universidad de Buenos Aires, Paraguay 2155, 5to piso, CP 1121 Buenos Aires, Argentina. Fax: +00-54-11-4508-3672. E-mail: dianakleiman@yahoo.com.ar.

**Hexachlorobenzene (HCB) is an organochlorine pesticide widely distributed in the environment. We have previously shown that chronic HCB exposure triggers apoptosis in rat thyroid follicular cells. This study was carried out to investigate the molecular mechanism by which the pesticide causes apoptosis in FRTL-5 rat thyroid cells exposed to HCB (0.005, 0.05, 0.5, and 5µM) for 2, 6, 8, 24, and 48 h. HCB treatment lowered cell viability and induced apoptotic cell death in a dose- and time-dependent manner, as demonstrated by morphological nuclear changes and the increase of DNA fragmentation. The pesticide increased activation of caspases-3, -8, and full-length caspase-10 processing. HCB induced mitochondrial membrane depolarization, release of cytochrome *c* and apoptosis-inducing factor (AIF), from the mitochondria to the cytosol, and AIF nuclear translocation. Cell death was accompanied by an increase in reactive oxygen species (ROS) generation. Blocking of ROS production, with a radical scavenger (Trolox), resulted in inhibition of AIF nuclear translocation and returned cells survival to control levels, demonstrating that ROS are critical mediators of HCB-induced apoptosis. The pesticide increased ERK1/2, JNK, and p38 phosphorylation in a time- and dose-dependent manner. However, when FRTL-5 cells were treated with specific MAPK inhibitors, only blockade of MEK1/2 with PD98059 prevented cell loss of viability, as well as caspase-3 activation. In addition, we demonstrated that HCB-induced production of ROS has a critical role in ERK1/2 activation. These results demonstrate for the first time that HCB induces apoptosis in FRTL-5 cells, by ROS-mediated ERK1/2 activation, through caspase-dependent and -independent pathways.**

***Key Words:*** **FRTL-5 cells; hexachlorobenzene; apoptosis; reactive oxygen species; ERK1/2.**

Hexachlorobenzene (HCB) is a widespread environmental pollutant that persists in the environment, bioaccumulates through the food chain, and has detrimental biological effects. Although the use of HCB was discontinued in most countries in 1970s, it is still released into the environment as a byproduct in several industrial processes. HCB exposure is associated with a broad spectrum of toxic effects, including endocrine disruption, immunological disorders, neurological symptoms, and thyroid dysfunctions (ATSDR, 2002). Alterations in thyroid metabolism and a risk excess of thyroid cancer have been reported in human populations exposed to organochlorinated compound mixtures with a high content of HCB (Grimalt *et al*., 1994; Meeker *et al*., 2007). Under normal circumstances, tissue homeostasis is a perfectly choreographed process balancing prosurvival and death signals. We have reported previously that HCB triggers apoptosis in rat thyroid without alterations in thyroid follicular cell proliferation (Chiappini *et al*., 2009). However, the molecular signaling mechanisms, underlying HCB-induced apoptosis in thyroid cells, are poorly documented.

Caspases, the key effectors of apoptosis, can be activated by intrinsic and extrinsic stimulus. The intrinsic pathway is initiated intracellularly by various forms of cellular stress, such as generation of reactive oxygen species (ROS), and involves the release of proapoptotic proteins such as cytochrome *c*, apoptosis-inducing factor (AIF), endonuclease G, and others, from mitochondria to the cytosol. Once released, cytochrome *c* interacts with the apoptotic activator factor-1 and, in concert with caspase-9, forms the apoptosome, and triggers the activation of caspases-3, -6, and -7, leading to apoptotic cell death (Kroemer *et al*., 2007). When AIF is released from the mitochondria in response to apoptotic stimuli, it becomes an active executioner of the cells by causing condensation of chromatin in the nuclei and large-scale fragmentation of DNA (Norberg *et al*., 2010).

The extrinsic apoptotic pathway is initiated by the activation of death receptors, such as the TNF-α receptor and Fas, as well as caspase-8 and -10. Activated caspase-8 can directly activate caspase-3 and/or induce cleavage of the proapoptotic Bcl-2 family member, Bid, to truncated Bid, which is translocated to the mitochondria, prompting cytochrome *c* release (Guicciardi

and Gores, 2005). Many xenobiotics, such as pesticides, may cause oxidative stress, leading to the generation of ROS and alterations in antioxidant enzyme systems. An *in vivo* oxidative stress condition has been reported in liver from HCB-treated rats (Almeida *et al.*, 1997; Ezendam *et al.*, 2004). ROS have been reported to induce alterations in mitochondrial membrane lipids, thereby inducing mitochondrial membrane permeability transition and the collapse of mitochondrial membrane potential ($\Delta\psi$m). It has been postulated that ROS may play a dual role in apoptosis, either as activators of permeability transition or as a consequence of this transition, depending on the death stimulus (Green and Reed, 1998). ROS generation has also been described to activate all mitogen-activated protein kinases (MAPK) cascades in response to oxidant injury, and they can, therefore, have an impact on cell survival and cell death (Cagnol and Chambard, 2010). Although ERK1/2 is generally associated with cell proliferation and growth, ERK1/2 activation is now thought to contribute to apoptosis as well (Cagnol and Chambard, 2010). JNK and p38 pathways are stimulated by genotoxic agents and cytokines mediating the stress response, growth arrest, and apoptosis (Xia *et al.*, 1995). However, it has been reported that more complex roles of these MAPK pathways exist to transmit other ultimately distinct cellular effects (Chuang *et al.*, 2000). It has been reported that the requirement for either JNK or p38 MAPK in stress-induced apoptosis varies depending on the cell type and on the context in which the kinase is activated (Frasch *et al.*, 1998). The aim of this study was to investigate the molecular mechanism of action involved in HCB-induced cell death in FRTL-5 cell line. Research in the understanding of pesticide-induced cytotoxicity is necessary for a complete understanding of the human health consequences to pesticide exposure in order to establish improved usage regulations and reduction of exposure risk.

## MATERIALS AND METHODS

*Chemicals.* HCB (> 99% purity, commercial grade), Coons' modified F-12 medium, thyroid-stimulating hormone (TSH), insulin, hydrocortisone, transferrin, somatostatin, glycyl-L-histidyl-L-lysine, protease inhibitors, PMSF, aprotinin, leupeptin, and pepstatin, (3-(4,5-dimethylthiazol-2-yl)-2,5-diphenyltetrazolium bromide) (MTT), 2′,7′-dichlorfluorescein-diacetate (DCHF-DA), and the specific inhibitors (2-(2-amino-3-metoxifenyl)-4H-1-benzopiran-4-one [PD98059], 1,9-pyrazoloanthrone, anthrapyrazolone [SP600125], the pyridinyl imidazole compound [SB203580], and antioxidant 6-hydroxy-2,5,7,8-tetramethylchroman-2-carboxylic acid [Trolox]) were purchased from Sigma Chemical Co. (St Louis, MO). Anti-caspase-8 (p18) and anti phospho-c-jun (Ser 63/73) antibodies were purchased from Santa Cruz Biotechnology (Santa Cruz, CA). Anti-caspase-3 (p-17), anti-caspase-10 (detects endogenous levels of full-length (FL) caspase-10, anti-p38 MAPK, anti p44/42 MAPK, anti-phopho-p38 MAPK, anti-phospho-p44/42 MAPK, anti-phospho SAPK/JNK (Thr183/Tyr 185), and anti SAPK/JNK primary antibodies were obtained from Cell Signaling Technology Inc., (Beverly, MA). Anti-cytochrome *c* was purchased from BD Biosciences-Pharmingen (Buenos Aires, Argentina). Anti-β-actin was from Abcam Inc. (Cambridge, MA). Dulbecco's Modified Eagle's Medium (DMEM) was obtained from Invitrogen Life Technology (Carlsbad, CA). DMEM-high glucose, without phenol-red, cell culture media supplements, and antibiotics were all purchased from PAA Laboratories GmbH (Pasching, Austria). The enhanced chemiluminescence kit (ECL) was from GE Healthcare Life Sciences (Buckinghamshire, UK). Terminal desoxynucleotidyl transferase–mediated desoxyuridine triphosphate nick end-labeling (TUNEL) label mix (nucleotide mix, containing fluorescein-dUTP and dNTP) was purchased from Roche S.A. (Buenos Aires, Argentina). MitoTracker Red 580 was from Molecular Probe (Eugene, OR). All other reagents used were of analytical grade.

*Cell culture.* Fisher rat thyroid cell line (FRTL-5) is derived from Fisher rat thyroids and has an obligate requirement for TSH for growth in cell culture. FRTL-5 cells were routinely cultured in Coons' modified F-12 medium (50%) and DMEM-high glucose (50%), containing a six-hormone (6H) mixture composed of insulin (10 µg/ml), hydrocortisone (10nM), transferrin (5 µg/ml), glycyl-L-histidyl-L-lysine (10ng/ml), somatostatin (10ng/ml), and bovine TSH (1 mU/ml), and supplemented with penicillin (10,000 IU/ml), streptomycin (10mg/ml), amphotericin B (25 µg/ml), and 5% fetal bovine serum (FBS) in 5% $CO_2$-95% $O_2$ at 37°C in a humidified incubator until confluence. The medium was replaced with fresh medium every 2–3 days.

*Cell treatment for time-course and dose-response studies.* FRTL-5 cells were seeded in 100-mm dishes ($1.5 \times 10^6$ cells) in DMEM/F12 complete growth medium followed by overnight incubation to allow cells to attach. Afterwards, the medium was withdrawn and replaced with fresh serum- and TSH-free medium (5H medium without FBS), and 24h later, cells were exposed to HCB dissolved in absolute ethanol, according to the assay. Final ethanol concentration in each treatment was 0.5% and had no influence on the analyzed parameters. For time-course studies, cells were treated with 5µM HCB in DMEM/F12 complete growth medium or vehicle for 2, 6, 8, 24, and 48 h. For dose-response studies, cells were exposed for 6 or 8 h to HCB (0.005, 0.05, 0.5, and 5µM) in DMEM/F12 complete growth medium. Selected doses were in the same range as that found in serum from humans from a highly contaminated population (To-Figueras *et al.*, 1997). After HCB exposure, cells were washed twice with ice-cold PBS and processed according to the experiment.

*Subcellular fractionation.* FRTL-5 cells were washed thrice with ice-cold PBS and harvested in 5 volumes of lysis buffer containing 20mM (HEPES-KOH), 1mM EDTA, 1mM EGTA, 1mM dithiothreitol (DTT), 0.1mM PMSF, pH 7.5, 20 µg/ml aprotinin, 120µM leupeptin, and 12µM pepstatin. Nuclei were pelleted by centrifugation at 750 × g for 10min. The supernatant layer was centrifuged for 15 min at 10,000 × g to remove mitochondria. The resulting supernatant was used for cytosolic proteins. The nuclear pellet was resuspended in lysis buffer containing 0.5% Triton X-100, 0.15M NaCl, 20mM Tris-HCl, pH 7.4, 1mM EGTA, 1mM EDTA, 50mM NaF, 1mM PMSF, 2mM $Na_3VO_4$, 20 µg/ml aprotinin, 120µM leupeptin, and 12µM pepstatin, and the resulting suspension was used for the assay of nuclear proteins. Protein concentration was determined according to the study by Bradford (1976) using bovine serum albumin (BSA) as a standard.

*Cell treatment for inhibitor assays.* For assays performed in the presence of specific ERK1/2, JNK, and p38 inhibitors, cells were pretreated for 1h with 10µM of MEK inhibitor, PD98059, 50µM of JNK-specific inhibitor, SP600125, and 10µM of p38 MAPK inhibitor, SB203580, respectively. Five micromoles of HCB or vehicle was added to the media during the time indicated in the corresponding figures in the presence or absence of inhibitors, and then cells were washed with PBS.

*Assessment of cell death.* Cells with fragmented nuclear DNA were detected using the TUNEL. Briefly, FRTL-5 cells were exposed to HCB (0.005, 0.05, 0.5, and 5µM) or vehicle for 8 or 24 h. After treatment, the glass slides were washed with PBS and fixed with cold 10% ethanol. Then, the cells were treated with proteinase K (20 µg/ml) in 10mM Tris-HCl, pH 7.4, at room temperature during 30min. After that, cells were washed and permeabilized with 0.1% Triton X-100 and 0.1% sodium citrate in PBS for 8min. Then the cells were incubated in equilibrium buffer (200mM potassium cacodylate, pH 6.6, 25mM Tris-HCl, pH 6.6, 0.2mM DTT, 0.25 mg/ml BSA, and 2.5mM cobalt chloride) for 10min and then incubated with the reaction buffer, which contained the TUNEL label mix (nucleotide mix, containing fluorescein-dUTP and dNTP), and the enzyme terminal deoxynucleotidyl transferase (TdT) during 60min at

37°C. Cell nuclei were stained with Hoescht dye (5 µg/ml in PBS) for 10 min at room temperature. Later, cells were analyzed under a fluorescence microscope Olympus BX50 F-3 (Olympus Optical Co., Ltd, Japan). For negative controls, we omitted the TdT reaction step in the TUNEL method. Photographs were analyzed with Image–Pro Plus v4.5 (Media Cybernetics Inc.) software.

***Cell viability.*** The measurement of cell viability was evaluated by MTT colorimetric assay. This process requires active mitochondria, and even freshly dead cells do not cleave significant amounts of MTT. The cell viability and cell number are proportional to the value of absorbance measured by spectrophotometry at 570 nm. Briefly, $6 \times 10^3$ FRTL-5 cells were seeded in 96-well plates and maintained in DMEM/F12 complete medium for 24 h. The next day medium was removed, and TSH- and serum-free DMEM/F12 medium was added. Finally, cells were treated with HCB (0.005, 0.05, 0.5, and 5µM) or ETOH in complete DMEM/F12 medium for 2, 6, 8, 24, and 48 h, and MTT (0.5 mg/ml) solution dissolved in DMEM without phenol-red was added to each well and incubated for 1 h at 37°C. Formazan crystals were dissolved in 100 µl dimethyl sulfoxide, and the absorbance of the solution was measured at 570 nm using the microplate reader Synergy HT (Biotek Instruments, Inc.).

***Evaluation of apoptotic morphology by light microscopy.*** At the indicated times after HCB treatment, the cells were washed with PBS, and changes in cell morphology were examined by staining slides with the Hoechst dye (5µM/ml in PBS) reagent during 10 min at room temperature. After staining, the slides were dried thoroughly and rinsed in PBS, and nuclear morphology was observed using a fluorescence microscope, Olympus BX50 F-3 (Olympus Optical Co., Ltd), and images were analyzed with software Image–Pro Plus v4.5 (Media Cybernetics Inc.) software.

***Assay of ROS production.*** In order to determine the quantity of ROS produced by FRTL-5 cells, the $H_2O_2$ concentration within the cells was assayed using the DCFH-DA as a well-established compound to detect and quantify intracellular produced ROS. DCFH-DA is freely permeable across the membranes; upon entering the cell, the acetate groups are hydrolyzed, creating a membrane impermeable form of the dye (DCFH). Hydrogen peroxide and peroxidases produced by the cell oxidize DCFH to yield a quantifiable fluorogenic compound 2′,7′-dichlorofluorescein, representing the level of ROS present in the cell, which can be detected by fluorescent microscopy with excitation and emission settings at 488 and 525 nm, respectively.

FRTL-5 cells were seeded in 96-well plates and grown in complete DMEM/F12 medium for 24 h. Cells were incubated in 5H medium without FBS for 24 h at 37°C, then incubated with DCFH-DA (10µM) for 30 min, and exposed to HCB in DMEM without phenol-red for the indicated concentrations and periods. After the incubation time, relative fluorescence intensity was measured on a microplate reader Synergy HT (Biotek Instruments, Inc.). The recorded fluorescence was analyzed using image software Gen5 (Biotek Instruments, Inc.).

***Detection of mitochondrial membrane permeabilization.*** We have used a MitoTracker Red probe that is concentrated by active mitochondria. After HCB treatment in DMEM/F12 complete medium, mitochondria were labeled with 50nM Mito Tracker Red 580, in DMEM without phenol-red, for 30 min in the dark, then washed twice with PBS, and fixed with 4% formaldehyde solution during 15 min at 4°C. Finally, cells were incubated with Hoechst dye and analyzed under a fluorescence microscope, Olympus BX50 F-3 (Olympus Optical Co., Ltd). Images were analyzed with software Image–Pro Plus v4.5 (Media Cybernetics Inc.) software.

***Western blotting.*** Total cellular protein lysates and cytosolic or nuclei proteins were electrophoresed in 10–12% SDS-polyacrylamide gel (SDS-PAGE), prior to transfer to PVDF membranes (Millipore, Bedford, MA), in a semidry transfer cell at 18V for 1.5 h. Membranes were blocked overnight at 4°C with 5% nonfat dry milk-2.5% BSA in Tris buffer saline solution with Tween 20 (TBST) buffer (10mM Tris-HCl, pH 8.0, 0.5% Tween 20, 150mM NaCl). Membranes were incubated with rabbit polyclonal antibodies, anti-caspase-3 (1:500), FL anti-caspase-10 (1:500), anti-p44/42 MAPK (1:1000), anti-p38 MAPK (1:500), anti-p-JNK (1:500), anti-ERK1/2 (1:1000), and anti-JNK1 (1:500), and with mouse monoclonal antibodies, anti-caspase-8 (1:500), anti-cytochrome *c* (1:500),

anti-AIF (1:500), anti-p38 (1:500), and anti-β-actin (1:2000) overnight at 4°C. After incubation, membranes were washed five times with TBST, and the suitable peroxidase-conjugated antispecies-specific antibodies were used for protein detection. After washing, blots were reacted using ECL detection kit (Amersham Biosciences, Inc., UK) and quantified by scanning laser densitometry in a Fotodyne (Foto/Analyst), Gel-Pro Analyzer 3.1.

***Statistical analysis.*** Data are expressed as means ± SEM. Differences between treated and control groups were analyzed by one-way or two-way ANOVA at a 95% confidence interval, followed by Tukey or Bonferroni's *post hoc* test to identify significant differences between samples and their respective controls, after testing homogeneity of variance using Barlett's procedure. Differences between control and treated cells were considered significant when $p$ values were < 0.05. For each experiment, at least three independent assays were performed.

## RESULTS

### Effect of HCB on Cell Viability, Morphology, and Apoptosis

Recently, we have shown that HCB induces apoptotic cell death in rat thyroid (Chiappini *et al.*, 2009). The viability of FRTL-5 cells was determined by an MTT assay, which measures mitochondrial function and can detect the onset of cell death. FRTL-5 cells were treated with HCB (0.005, 0.05, 0.5, and 5µM) for 2, 6, 8, 24, and 48 h. Our results show that 0.5 and 5µM HCB caused a significant loss of cell viability (15–28%), respectively, after 8 h of treatment and thereafter until 48 h (Fig. 1A). At the lower doses, there was no cytotoxicity under pesticide exposure.

Morphological hallmarks of apoptosis in the nucleus are chromatin condensation and nuclear fragmentation. The abnormalities of cell morphology were examined using a fluorescence microscope after Hoechst staining. Our results show that HCB (0.5 and 5µM) treatment for 8 and 24 h induced a significant increase (58 and 115%) and (50 and 70%), respectively, in morphological changes such as condensation of nuclear chromatin along the perimeter of the nucleus; circular or oval nuclei became increasingly lobular and eventually fragment into multiple subnuclei (Fig.1B). On the other hand, 0.005 and 0.05µM HCB-treated cells did not present significant nuclear alterations in their shape or size and presented a uniform fluorescence with Hoescht dye.

TUNEL assay, based on labeling of DNA strand breaks generated during apoptosis, was further carried out to confirm the cell apoptosis–inducing activity of HCB. Apoptotic cell death was studied in response to 5µM HCB, which induced the highest loss of cell viability, as determined by the MTT assay. Figure 2A shows that many of the Hoechst-stained condensed nuclei were also positive to the TUNEL assay at 6, 8, and 24 h.

Because caspases play a very important role in early apoptosis, we investigated the activation of executive caspase-3 in response to HCB treatment. Caspase-3 is a key apoptotic executive caspase, being activated by proteolytic cleavage due to caspases-8, -10, and -9. Western blotting analysis of caspase-3 was performed using an antibody known to
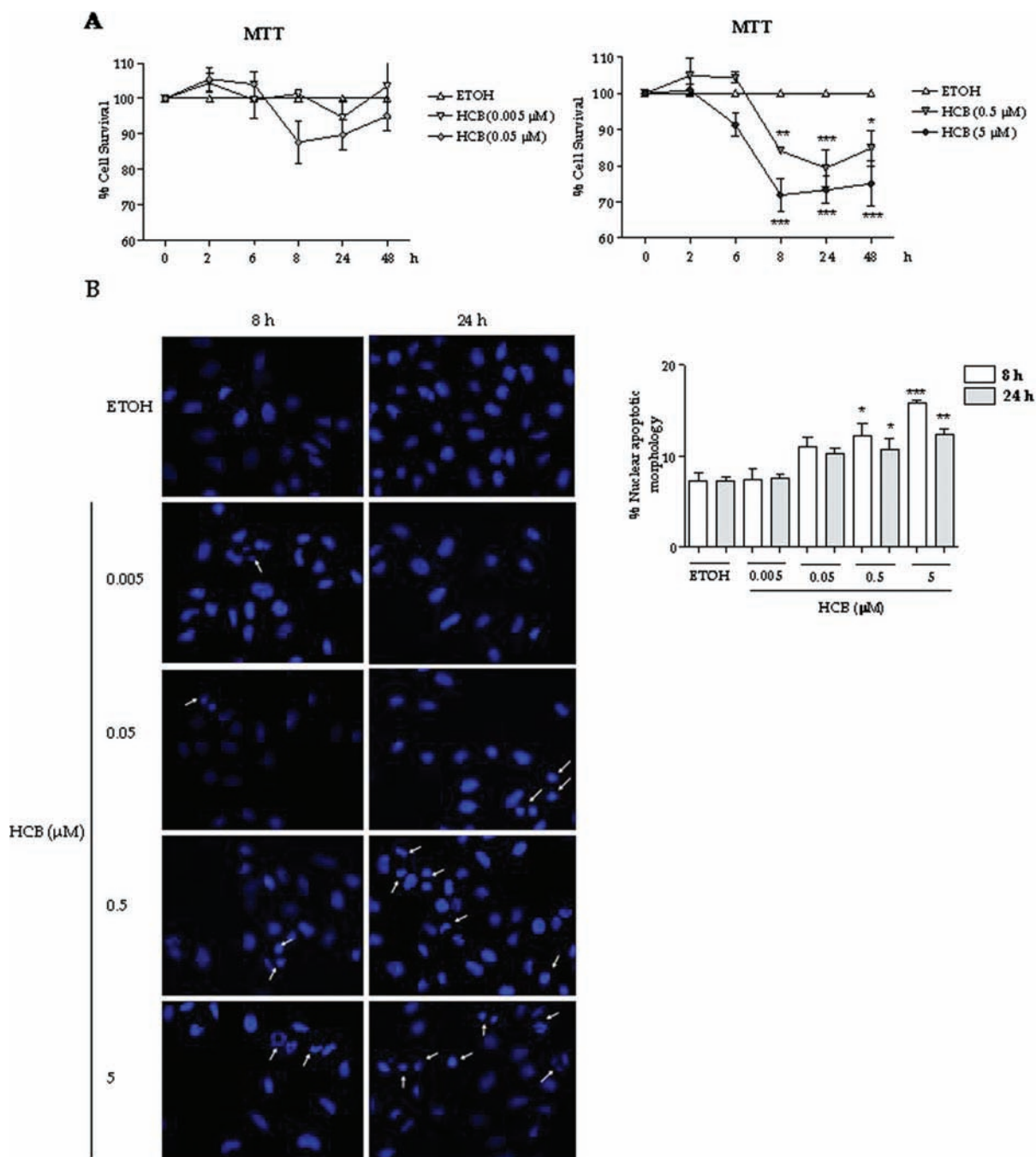
**FIG. 1.** HCB induces FRTL-5 cell death. (A) Effect of HCB on FRTL-5 cell survival. The viability of cells was evaluated using the viability MTT assay. Cells were treated with MTT (0.5 mg/ml) and incubated for 1 h at 37°C. Then the absorbance was measured at 570 nm, and the results were expressed as percentage of ETOH-treated cells. (B) Morphological changes induced by HCB. Cells were incubated for 8 or 24 h with HCB (0.005, 0.05, 0.5, and 5µM) or ETOH. Magnification ×400. Percentage of cells with nuclear apoptotic morphology was quantified. Arrows denote apoptotic morphological changes. Data are expressed as means ± SEM of three independent experiments. Asterisks indicate significant differences versus ETOH (*$p < 0.05$, **$p < 0.01$, ***$p < 0.001$). Statistical comparisons were made by one-way ANOVA with a 95% confidence interval followed by Tukey *post hoc* test to identify significant differences between mean values and indicated controls.

recognize the p17 activated form. Time-dependent studies showed that 5µM HCB treatment, during 6 and 8 h, resulted in the increase of active caspase-3 (160 and 500%), respectively, compared with ETOH-treated cells (Fig. 2B). These results

indicate that executioner caspase-3 is involved in the apoptotic cell death induced by HCB. We also examined dose-response effects of HCB treatment during 8 h on caspase-3 (p17) protein levels. Figure 2C shows that HCB (0.5 and 5µM) significantly
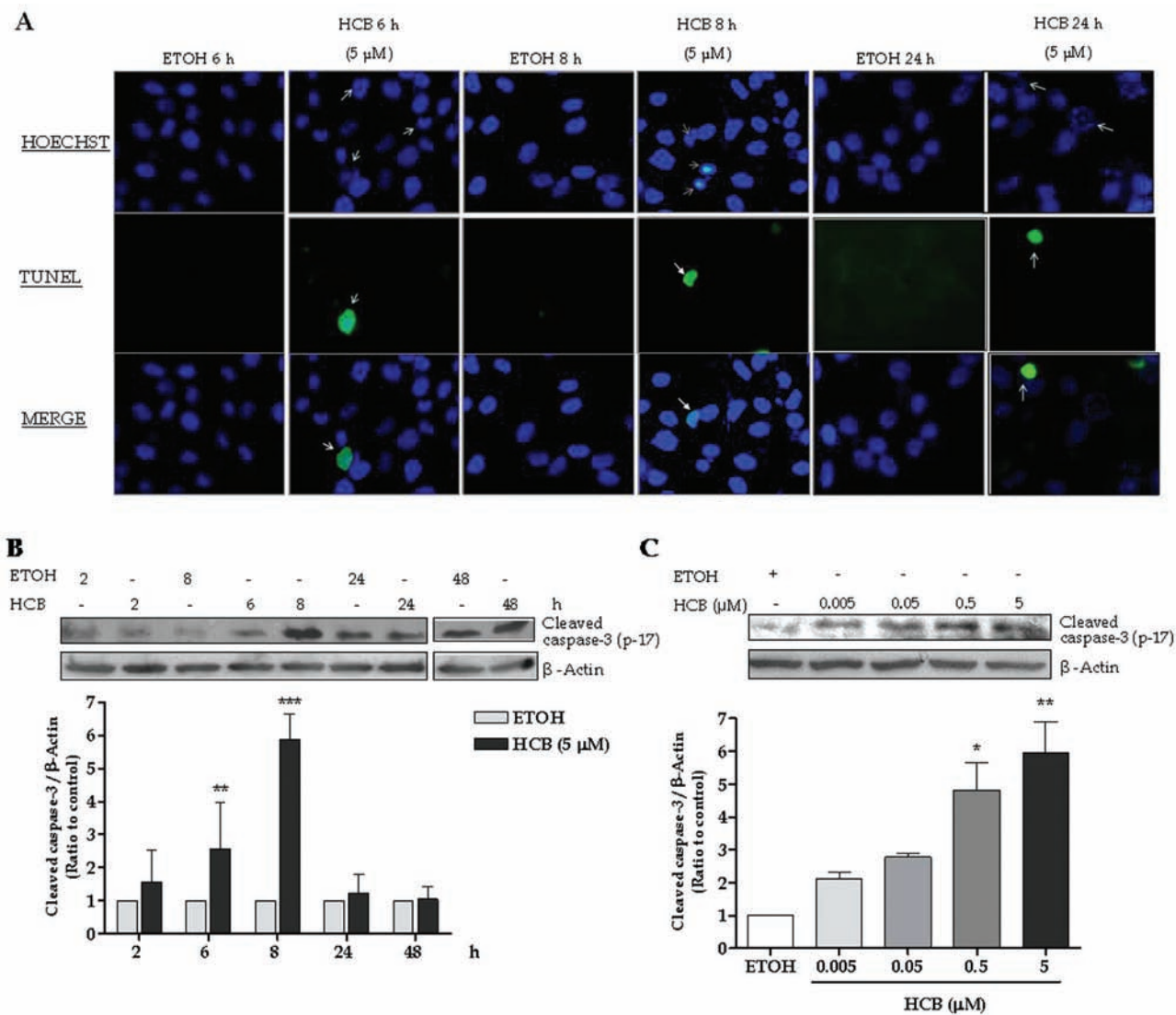
**FIG. 2.** HCB induced DNA fragmentation and activation of caspase-3. (A) Detection of *in situ* DNA breaks by TUNEL assay. Cells were exposed to 5µM HCB for 6, 8, and 24h. Magnification ×600. Arrows point to positive nuclei. (B) Time course of HCB effect on caspase-3 activation. FRTL-5 cells were treated with 5µM HCB for 2, 6, 8, 24, and 48h. (C) Dose-response effects of HCB on caspase-3 activation. Western blots from one representative experiment are shown in the upper panels. Quantification of cleaved caspase-3/β-actin ratio to control by densitometry scanning of the immunoblots is shown in the lower panels. Data are expressed as means ± SEM of three independent experiments. Asterisks indicate significant differences versus ETOH (*$p < 0.05$, **$p < 0.01$, ***$p < 0.001$). Statistical comparisons were made by one-way ANOVA with a 95% confidence interval followed by Tukey *post hoc* test to identify significant differences between mean values and indicated controls.

increased active caspase-3 protein levels (380 and 500%), respectively. Altogether, these results demonstrate that HCB decreased cell viability and induced apoptotic cell death in a time-and dose-dependent manner.

*HCB Triggered Activation of Initiator Caspases*

To detect whether other caspases were involved in HCB-induced apoptosis, cells were treated with 5µM HCB or ETOH for different periods of time. Activation of initiator caspase-8 was analyzed by Western blotting of the p18 fragment of processed caspase-8. Exposure to HCB resulted in the increase

of active caspase-8 protein levels (250, 300, and 140%), after 2, 6, and 8h, respectively, when compared with ETOH-treated cells (Fig. 3A). To evaluate dose-response effects of HCB on caspase-8 activation, FRTL-5 cells were treated with HCB during 8h. As shown in Figure 3B, HCB (0.05, 0.5, and 5µM) significantly increased active caspase-8 protein levels (150, 120, and 95%), respectively, showing a decreasing trend with higher HCB concentrations.

In order to evaluate whether initiator caspase-10 was involved in HCB-induced apoptosis, we determined decreases in FL caspase-10 protein levels by Western blotting, which
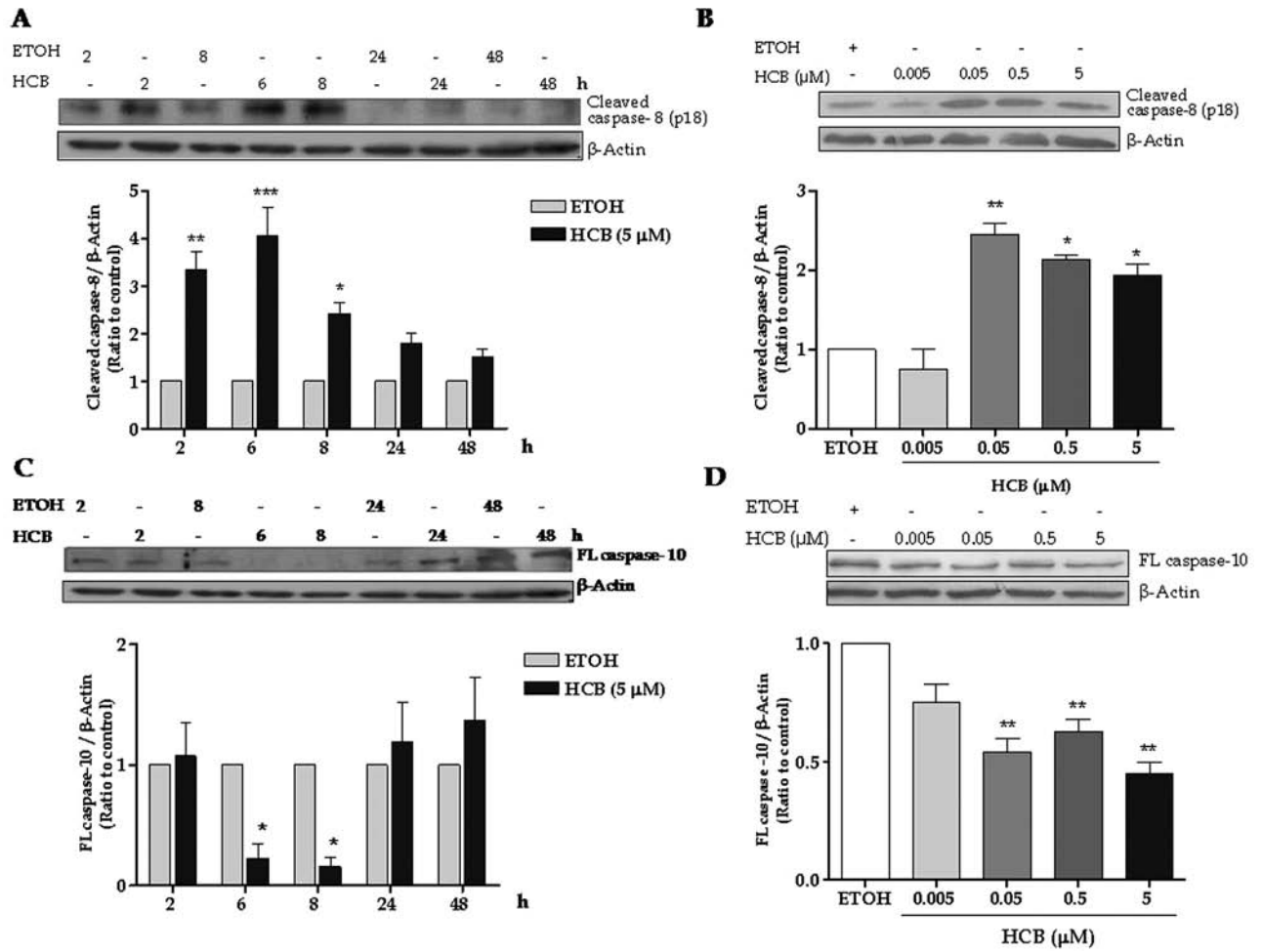
**FIG. 3.** HCB effect on caspase-8 and caspase-10 activation. Whole-cell lysates were prepared, and proteins were resolved by SDS-PAGE and blotted with specific antibodies. (A and C) Time-dependent studies; (B and D) dose-response effects. Western blots from one representative experiment are shown in the upper panels. Quantification of active caspase-8/β-actin and FL caspase-10/β-actin ratio to controls is shown in the lower panels. Data are expressed as means ± SEM of three independent experiments. Asterisks indicate significant differences versus ETOH (*$p < 0.05$, **$p < 0.01$, ***$p < 0.001$). Statistical comparisons were made by one-way ANOVA with a 95% confidence interval followed by Tukey *post hoc* test to identify significant differences between mean values and indicated controls.

correlates with active caspase-10 as reported by Kalli *et al.* (2003). Time-dependent studies showed that 5µM HCB decreased FL caspase-10 protein levels, 80 and 85% at 6 and 8 h, respectively, and then returned to control levels (Fig. 3C). To evaluate dose-response effects of HCB on caspase-10 activation, FRTL-5 cells were treated with HCB or ETOH during 8 h. As shown in Figure 3D, FL caspase-10 protein levels were significantly decreased (44, 37, and 53%) with HCB (0.05, 0.5, and 5 µM), respectively. Altogether these results indicate that both initiator caspase-8 and caspase-10 are activated in HCB-treated FRTL-5 cells.

*HCB Induces Release of Mitochondrial Apoptotic Factors*

To evaluate the time-course effects of HCB on cytochrome *c* and AIF release into the cytosol, cells were treated with the highest HCB dose (5µM) that induced caspase-3 activation. Cytochrome *c* release from the mitochondria was detected

by Western blotting in the cytosolic fraction of FRTL-5 cells treated with the pesticide. The time-course analysis showed that HCB induced (260%) the release of cytochrome *c* from the mitochondria into the cytosol at very early times of treatment (2 h) and returned to ETOH levels following longer HCB exposure (Fig. 4A). We further used Western blot analysis to identify AIF, another signaling molecule that might be involved in the intrinsic apoptotic cascade. As shown in Figure 4B, AIF cytosolic protein levels were readily increased (129%) at 2 h, and this effect persisted up to 48 h. Cytosolic AIF protein levels were corrected for mitochondrial AIF contamination using a specific mitochondrial complex III antibody. We also examined whether released AIF translocates into the nucleus. Western blot analysis show that 5µM HCB increased nuclear AIF protein levels (150, 180, 130, and 60%) after 6, 8, 24, and 48 h of exposure, respectively (Fig. 4C).
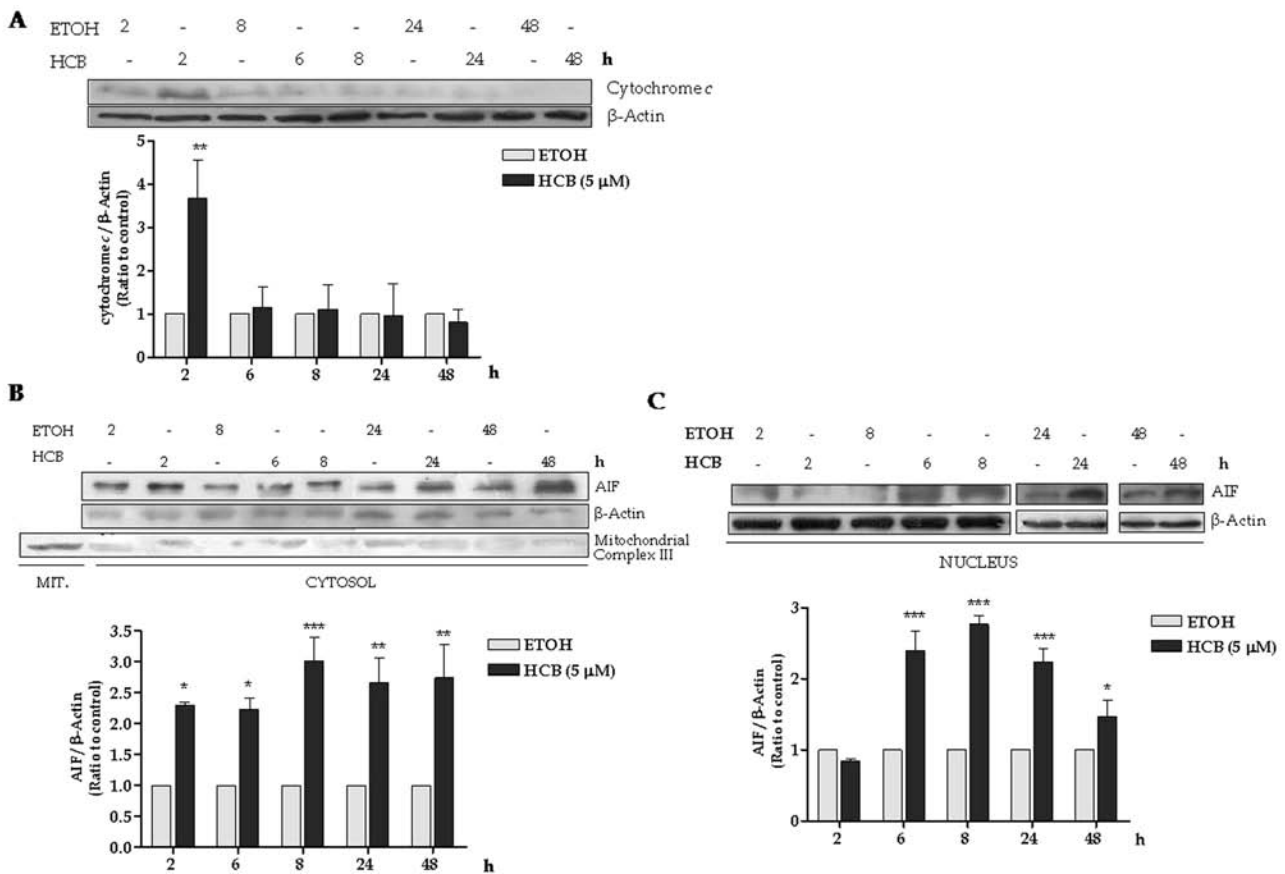
**FIG. 4.** HCB-induced apoptosis involves cytochrome $c$ and AIF release from the mitochondria. (A and B) Cytochrome $c$, AIF, and β-Actin protein levels were determined by immunoblotting in the cytosolic fraction. (C) AIF and β-actin protein levels were determined in the nuclear fraction. Western blots from one representative experiment are shown in the upper panels. Quantification of cytochrome $c$/β-actin and AIF/β-actin ratio to control by densitometric scanning of the immunoblots is shown in the lower panels. Data are expressed as means ± SEM of three independent experiments. Asterisks indicate significant differences versus their corresponding controls (*$p < 0.05$, **$p < 0.01$, ***$p < 0.001$). Statistical comparisons were made by one-way ANOVA with a 95% confidence interval followed by Tukey *post hoc* test to identify significant differences between mean values and indicated controls.

### HCB-Induced Oxidative Stress

Because accumulating evidence supports that intracellular ROS are produced by toxic chemicals, and oxidative stress has been associated with apoptosis, we next determined whether HCB stimulates ROS generation in FRTL-5 cells. In this study, intracellular oxidized state was measured using a sensitive fluorescent assay method, with DCFH-DA. FRTL-5 cells were treated with 5µM HCB during 2, 3, 4, and 5h, and DCFH-DA-derived fluorescence was measured. As shown in Figure 5A, HCB significantly increased intracellular ROS levels (52%) as early as 2h, reaching a maximal level (320%) over ETOH-treated cells, at 4h, followed by a decline of fluorescence within 5h (226%). Dose-response studies showed that treatment of FRTL-5 cells with HCB (0.5 and 5µM) increased ROS content (109 and 90%), respectively, when compared with ETOH-treated cells (Fig. 5B).

To further evaluate the involvement of ROS in HCB-induced cytotoxicity, we examined the effect of Trolox, a radical scavenger and metal ion chelator, on cells viability. Cells were preincubated during 30min with 100µM Trolox and then incubated with 5µM HCB or ETOH during 24h. As shown in Figure 5C, preincubation with the radical scavenger returned cell viability to ETOH levels. To confirm that ROS generation was impeded by the antioxidant, FRTL-5 cells were preincubated with 100µM Trolox, followed by 5µM HCB during 4h. Figure 5D shows that Trolox treatment impeded HCB-induced ROS generation.

To determine whether ROS were involved in nuclear AIF translocation, FRTL-5 cells were preincubated with 100µM Trolox for 30min and then treated with 5µM HCB for 8h. Western blot analysis showed that Trolox decreased AIF nuclear protein content, indicating that ROS are involved in AIF nuclear translocation (Fig. 5E). Densitometric scanning of the immunoblot is shown in Supplementary figure 1.

### Mitochondrial Membrane Permeabilization

Disruption of mitochondrial integrity is one of the early events leading to apoptosis. To assess whether HCB affects the function
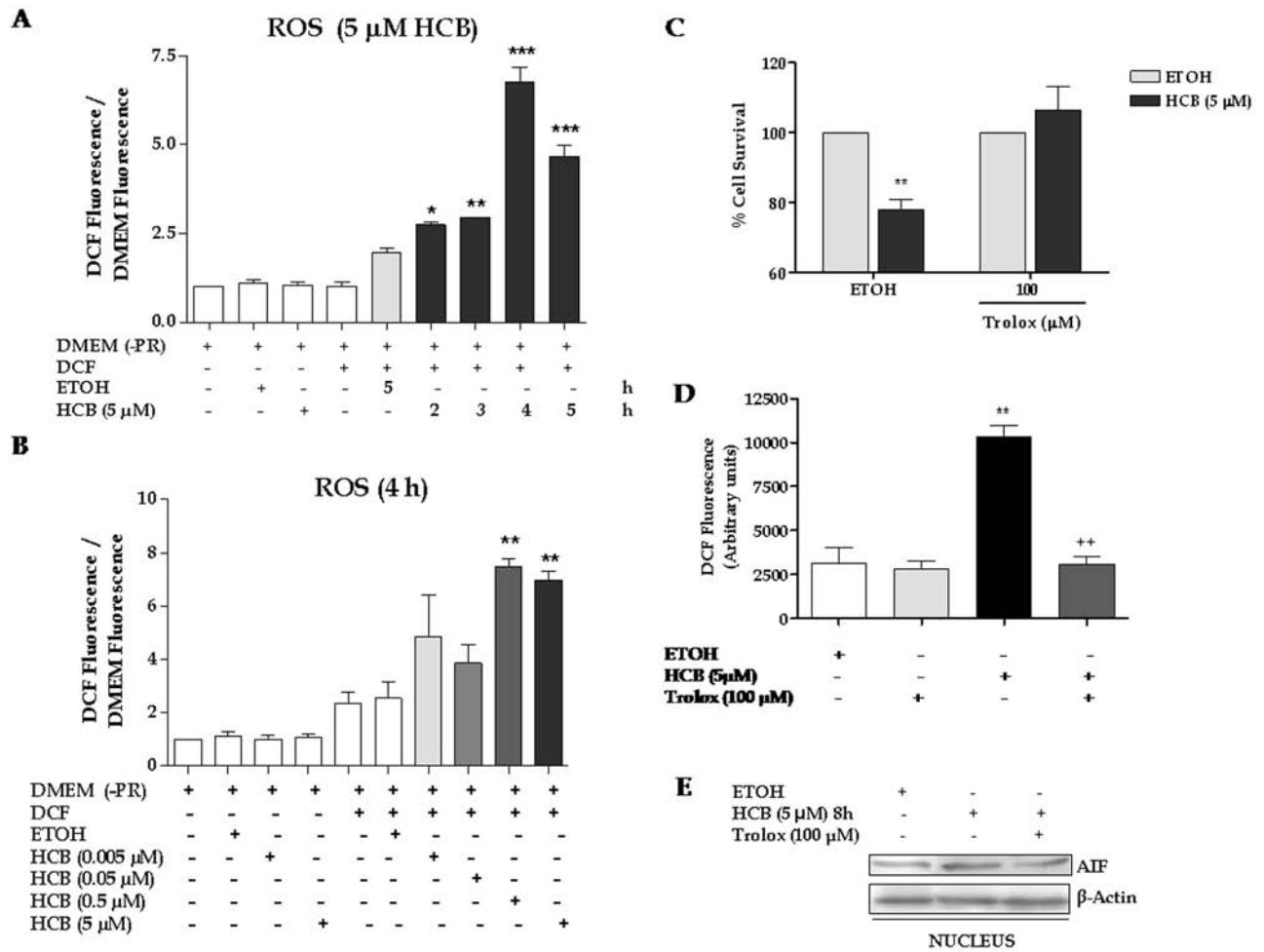
**FIG. 5.** Effect of HCB on intracellular ROS content. Levels of ROS produced by the cells were measured using ROS reactive fluorescence probe DCFH-DA. FRTL-5 cells were cultured with 10μM DCFH-DA for 30 min at 37°C and treated with HCB for the times and doses indicated in the text. Results were expressed as the ratio of DCF fluorescence/DMEM fluorescence under each treatment. (A) Time-dependent HCB effects; (B) dose-dependent HCB effects. (C) Role of ROS in HCB-induced cytotoxicity. Cell survival was evaluated with MTT assay; (D) effect of Trolox on ROS generation. (E) Role of ROS on AIF nuclear transloca-tion. Western blot of nuclear proteins were resolved by SDS-PAGE and blotted for AIF. Data are expressed as means ± SEM of three independent experiments. Asterisks indicate significant differences versus ETOH-treated cells (*$p < 0.05$, **$p < 0.01$, ***$p < 0.001$). Crosses indicate significant differences versus HCB, ++$p < 0.01$). Statistical comparisons were made by one-way ANOVA with a 95% confidence interval followed by Tukey *post hoc* test to identify significant differ-ences between mean values and indicated controls.

of mitochondria, dynamic changes of the mitochondrial popula-tion of FRTL-5 cells were analyzed by employing fluorogenic MitoTracker Red probe. As shown in Figure 6, exposure to HCB (0.05 and 0.5μM) for 6 h resulted in a significant increase in the fragmented mitochondria by approximately 240 and 288%, respectively. When cells were treated with 5μM HCB, the fluo-rochrome was hardly retained inside the mitochondria. These results suggest that the highest HCB dose resulted in a signifi-cant decrease of mitochondrial membrane potential (Δψm).

*HCB Action on ERK1/2, JNK1, and p38 MAPK Phosphorylation*

The MAPK family is involved in processes that induce cell death. In view of this evidence, the effects of HCB on the

phosphorylation of ERK1/2, JNK1, and p38 MAPK were evalu-ated. To evaluate time-response effects, FRTL-5 cells were first treated with 5μM HCB or ETOH for different periods of time. Total cell lysates were electrophoresed, and phosphorylation of ERK1/2, JNK1, and p38 MAPK was measured by Western blot analysis. Increased ERK1 and ERK2 phosphorylation appeared as early as 2 h (310 and 520%), respectively, and persisted for at least 24 h (200 and 183%), respectively. Total ERK1/2 protein levels were not modified (Fig. 7A). To evaluate dose-response effects of HCB on MAPK activation, FRTL-5 cells were incu-bated with different HCB doses or ETOH for 8 h. Our results showed that HCB (0.5 and 5μM) significantly enhanced ERK1 (262 and 450%) and ERK2 phosphorylation (390 and 466%) with HCB (0.5 and 5μM), respectively (Fig. 7B).
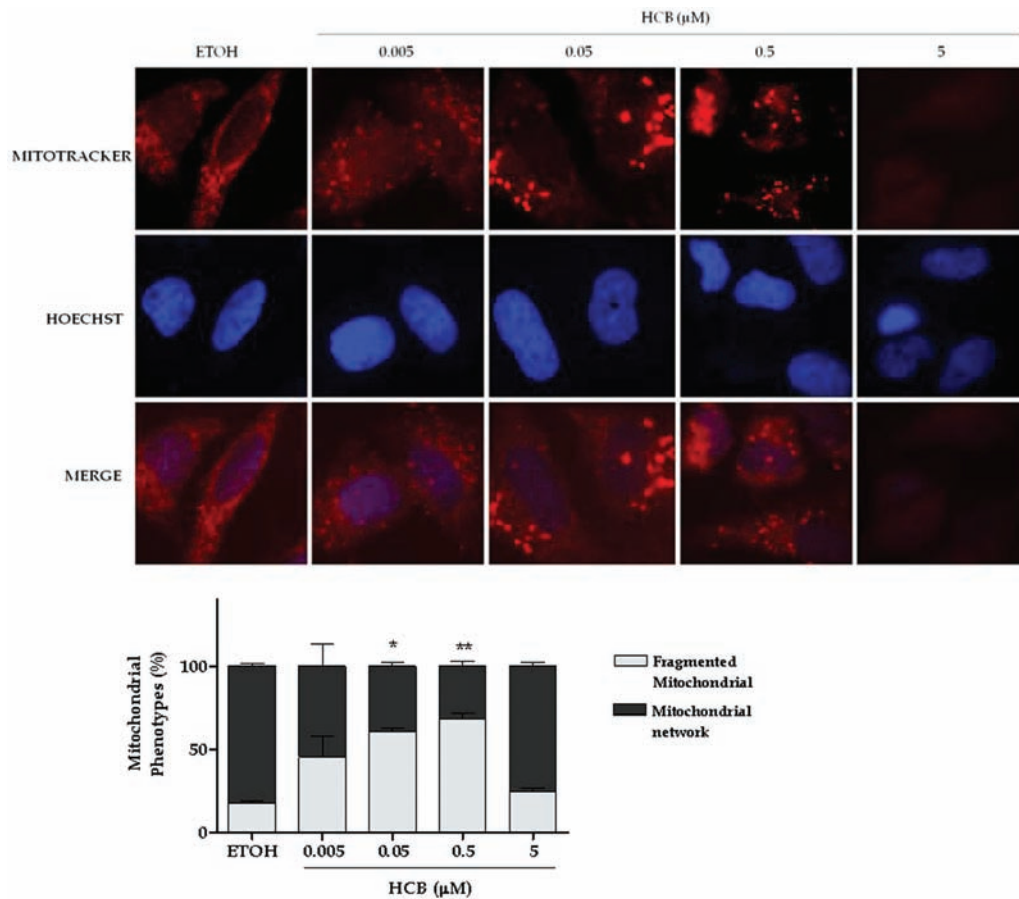
**FIG. 6.** HCB induces mitochondrial membrane permeabilization. FRTL-5 cells were treated with HCB (0.005, 0.05, 0.5, and 5μM) or ETOH for 6h, followed by the addition of the MitoTracker Red 580 probe. Cells were treated as indicated under Materials and Methods section. Magnification ×1000. Data are expressed as means ± SEM of three independent experiments. Asterisks indicate significant differences versus their corresponding controls (*$p < 0.05$, **$p < 0.01$). Statistical comparisons were made by one-way ANOVA with a 95% confidence interval followed by Tukey *post hoc* test to identify significant differences between mean values and indicated controls.

JNK was evaluated with a specific antibody that recognizes JNK1, 2, and 3. However as JNK2 and 3 band was feeble, only JNK1 isoform was analyzed. As shown in Figure 8A, JNK1 phosphorylation increased (160, 130, and 157%) at 2, 6, and 8h, respectively, after 5μM HCB exposures, returning toward baseline levels by 24 and 48h. Phospho-JNK1/JNK1 ratio was also increased (200, 75, and 132%) when cells were treated with HCB (0.05, 0.5, and 5μM) for 8h, respectively (Fig. 8B).

By contrast, time-course studies demonstrated that 5μM HCB treatments did not alter p38 MAPK phosphorylation (Fig. 9A). However, lower HCB concentrations (0.05 and 0.5μM) induced p38 phosphorylation (202 and 103%), respectively, when cells were exposed for 8h (Fig. 9B). Interestingly, a transient increase in phosphorylated p38 MAPK protein levels was observed after 15min of 5μM HCB exposure (Fig. 9C).

*Roles of ERK1/2, JNK1, and p38 MAPK on cell Viability*

In order to verify whether ERK1/2, JNK1, and p38 MAPK are involved in HCB-induced loss of cell viability, we examined the effects of specific MAPK inhibitors. When cells were pretreated during 1h, with increasing concentrations of PD98059 (10, 20, and 30μM), a specific MEK1 inhibitor, followed by 8h of exposure to 5μM HCB, ERK1/2 phosphorylation was decreased to ETOH levels (Fig. 10A). We further explored the potential role of ERK1/2 on cell viability under HCB treatment. Our results showed that 10μM PD98059 restored cell viability to ETOH values, indicating that ERK1/2 acts as an important mediator of the proapoptotic effect of HCB (Fig. 10B). Furthermore, we examined whether ERK1/2 acts upstream of caspase-3 activation, during HCB-induced apoptosis. As shown in Figure 10C, pretreatment with PD98059 returned active caspase-3 protein levels to ETOH values. These results indicate that ERK1/2 signaling precedes caspase-3 activation in FRTL-5 cells after HCB treatment.

To evaluate dose-response effect of the pharmacological inhibitor of JNK, SP600125, on c-jun phosphorylation, cells were pretreated with 25 and 50μM SP600125 for 1h, followed by 6h of treatment with 5μM HCB or ETOH. Phosphorylated-c-jun
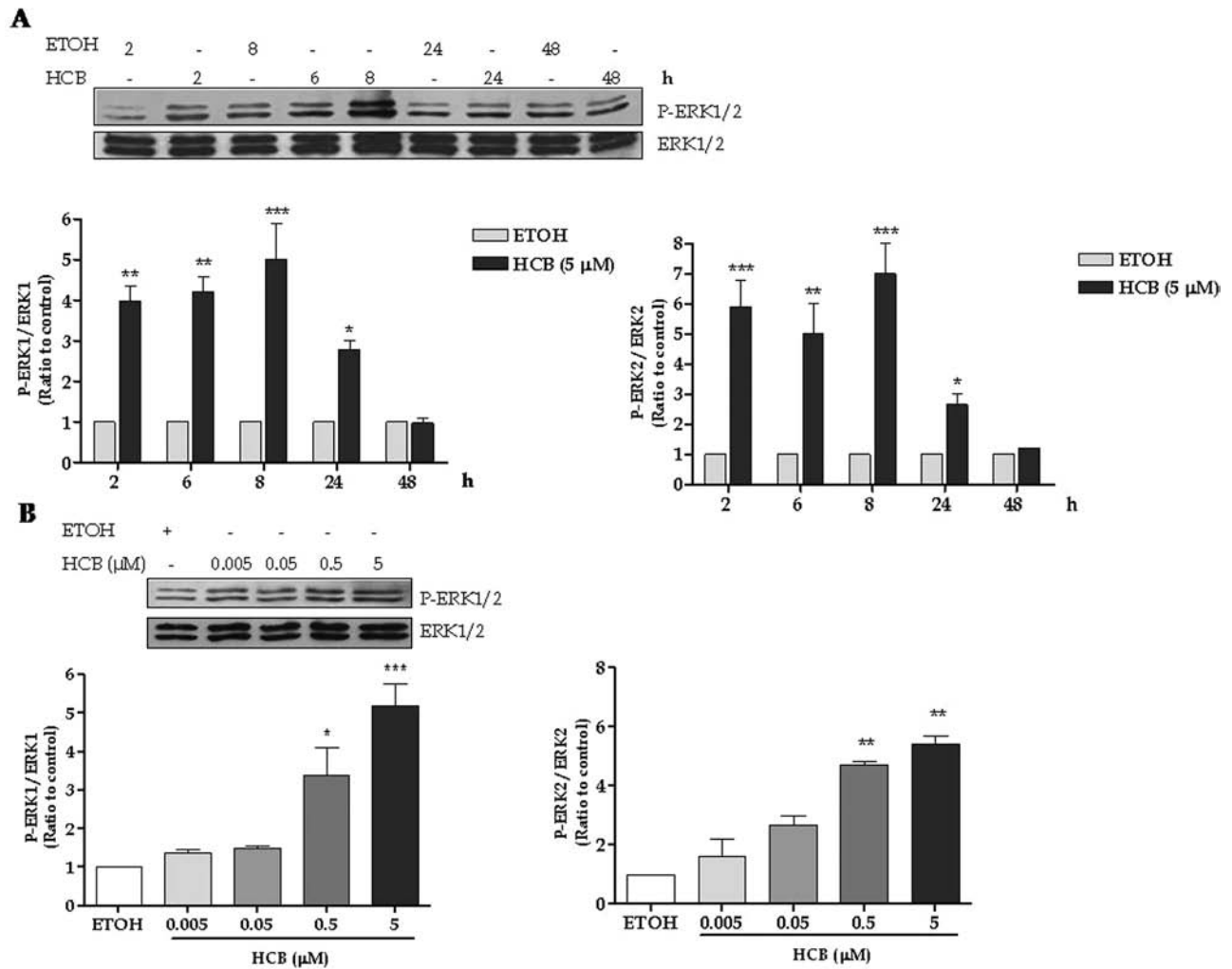
**FIG. 7.** HCB induces ERK1/2 phosphorylation. Whole-cell lysates were prepared, and proteins were resolved by SDS-PAGE and blotted with the corresponding specific antibodies. Western blots from one representative experiment are shown in the corresponding upper panels. Densitometric scanning of the immunoblots is shown in the lower panels. (A) Time course of HCB effect on ERK1 and ERK2 activation. Quantification of P-ERK1/ERK1 and P-ERK2/ERK2 ratio to control. (B) Dose-response effect of HCB on ERK1 and ERK2 activation. Quantification of P-ERK1/ERK1 and P-ERK2/ERK2 ratio to control. Data are expressed as means ± SEM of three independent experiments. Asterisks indicate significant differences versus ETOH-treated cells. (*$p < 0.05$, **$p < 0.01$, ***$p < 0.001$). Statistical comparisons were made by one-way ANOVA with a 95% confidence interval followed by Tukey *post hoc* test to identify significant differences between mean values and indicated controls.

was evaluated by immunoblot. As shown in Figure 10D, 50μM SP600125 returned HCB-induced c-jun phosphorylation to control values. The possible involvement of JNK1 on HCB-induced cytotoxic effect was studied, preincubating FRTL-5 cells with 50μM SP600125 for 1h, followed by 24h of 5μM HCB or ETOH exposure, in the presence of the inhibitor. Our result showed that cell viability was not restored, indicating that JNK1 is not involved in HCB-induced apoptosis (Fig. 10E).

We further examined whether the transient activation of p38 MAPK induces cell death. The effective dose of p38 kinase inhibitor was assayed incubating FRTL-5 with 10 and 15μM SB203580, followed by 15 min of 5μM HCB. Figure 10F shows that 10μM SB203580 inhibited p38 phosphorylation. The

possible involvement of p38 MAPK on HCB-induced loss of cell viability was assayed incubating FRTL-5 cells with 10μM SB203580, followed by 24h of 5μM HCB or ETOH exposure. As shown in Figure 10G, cell viability was not restored in the presence of p38 MAPK inhibitor. We have previously demonstrated that MAPK inhibitors did not alter cell survival (data not shown). Densitometric scanning of Figures 10A, C, D, and F are shown in Supplementary figure 2.

### ROS Mediate HCB-Induced Activation of ERK1/2

One type of stress that induces potential activation of MAPK pathways is the oxidative stress caused by ROS (Cagnol and Chambard, 2010). To investigate ROS effect on HCB-induced
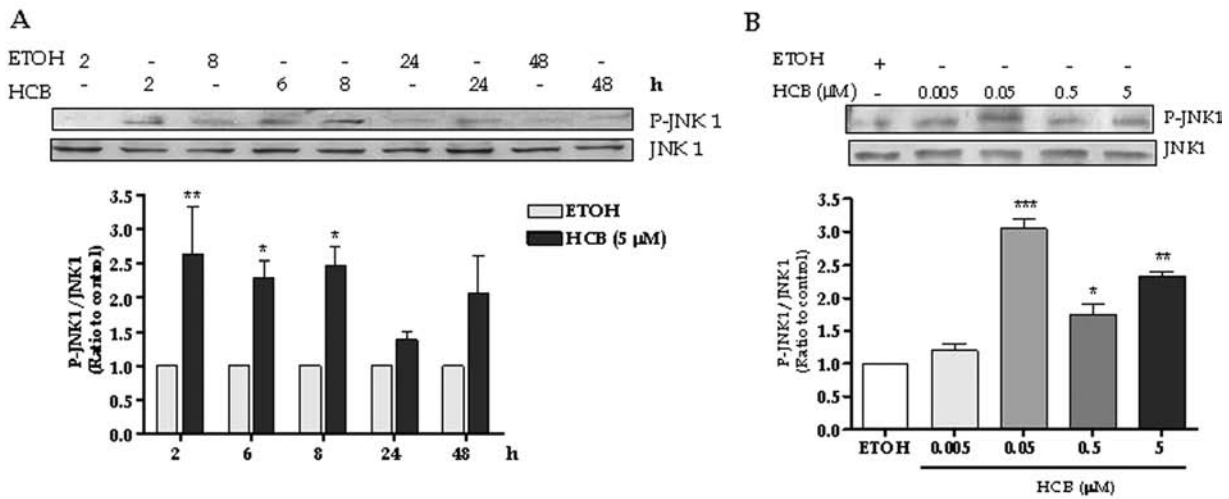
**FIG. 8.** HCB induces JNK1 phosphorylation. Whole-cell lysates were prepared, and proteins were resolved by SDS-PAGE and blotted with the corresponding specific antibodies. Western blots from one representative experiment are shown in the corresponding upper panels. Densitometric scanning of the immunoblots is shown in the lower panels. (A) Time course of HCB effect on JNK1 activation. Quantification of P-JNK1/JNK1 ratio to control. (B) Dose-response effect of HCB on JNK1 activation. Quantification of P-JNK1/JNK1 ratio to control. Data are expressed as means ± SEM of three independent experiments. Asterisks indicate significant differences versus ETOH-treated cells. ($*p < 0.05$, $**p < 0.01$, $***p < 0.001$). Statistical comparisons were made by one-way ANOVA with a 95% confidence interval followed by Tukey *post hoc* test to identify significant differences between mean values and indicated controls.

ERK1/2 activation, FRTL-5 cells were pretreated with $100\mu M$ Trolox, followed by $5\mu M$ HCB or ETOH for 8 h in the presence of the antioxidant. Our results showed that pretreatment with Trolox decreased ERK1/2 phosphorylation in total cell lysates, indicating that HCB induces activation of ERK1/2 through a mechanism dependent on ROS generation (Fig. 11).

### DISCUSSION

Apoptotic processes are of widespread biological significance, being involved in development, differentiation, proliferation/homoeostasis, regulation and function of the immune system, and the removal of defective and, therefore, harmful cells. However, little is known about the mechanisms and regulation of apoptotic signaling in thyroid cells. The results of this study are relevant because increasing evidence suggests that apoptosis plays an important role in the pathogenesis of autoimmune and proliferative thyroid diseases (Tsatsoulis, 2002).

In a previous work, we have demonstrated that doses of HCB that do not disrupt thyroid economy induce apoptosis in rat thyroids (Chiappini *et al.*, 2009). Herein, we have demonstrated that HCB (0.5 and $5\mu M$) induced loss of cell viability in FRTL-5 cell line. Therefore, we sought to identify the molecular mechanism of HCB-induced cell death in FRTL-5 cells treated with HCB at concentrations in the range of that found in serum from humans in a highly contaminated population ($0.004–3.34\mu M$) (To-Figueras *et al.*, 1997). TUNEL assay and nuclear morphological changes revealed that there was a significant percentage of apoptosis when FRTL-5 cells were

exposed to the pesticide. Activation of caspase-3, which is a prominent marker of apoptosis, was also induced by HCB. Altogether, these results suggest that apoptosis is the major mechanism of HCB-induced loss of cell viability. In addition, we have demonstrated that the pesticide did not alter cell proliferation (results not shown). Similarly we have previously shown that cell proliferation is not altered in thyroids from HCB-treated rats (Chiappini *et al.*, 2009).

Activation of caspases such as caspase-8, and caspase-10, which are regulatory elements in the extrinsic pathway, was also induced by the pesticide. Caspase-8 activation occurs at an earlier time point than caspase-3, which might be consistent with an upstream initiator role for caspase-8. Activation of caspase-8 and -10 does not necessarily imply involvement of death receptors. In this respect, it has been reported that the extrinsic pathway to apoptosis is not involved in cytotoxic drug–induced caspase-8 and -10 activation that occurs downstream of the mitochondria in tumor cells (Filomenko *et al.*, 2006). However, recent results of our laboratory have demonstrated that HCB-induced apoptosis in rat liver involves signals emanating from death receptors and from the mitochondria (Giribaldi *et al.*, 2011). Although our results suggest that caspase-8 and -10 might be involved in HCB-induced apoptosis in FRTL-5 cells, further studies would be necessary to clarify whether death receptors are involved.

Mitochondria are central to many forms of cell death, usually via the release of proapoptotic proteins from the mitochondrial intermembrane space. In healthy cells, mitochondria continually divide and fuse to form a dynamic interconnecting network. Recent work shows that proteins involved in mitochondrial
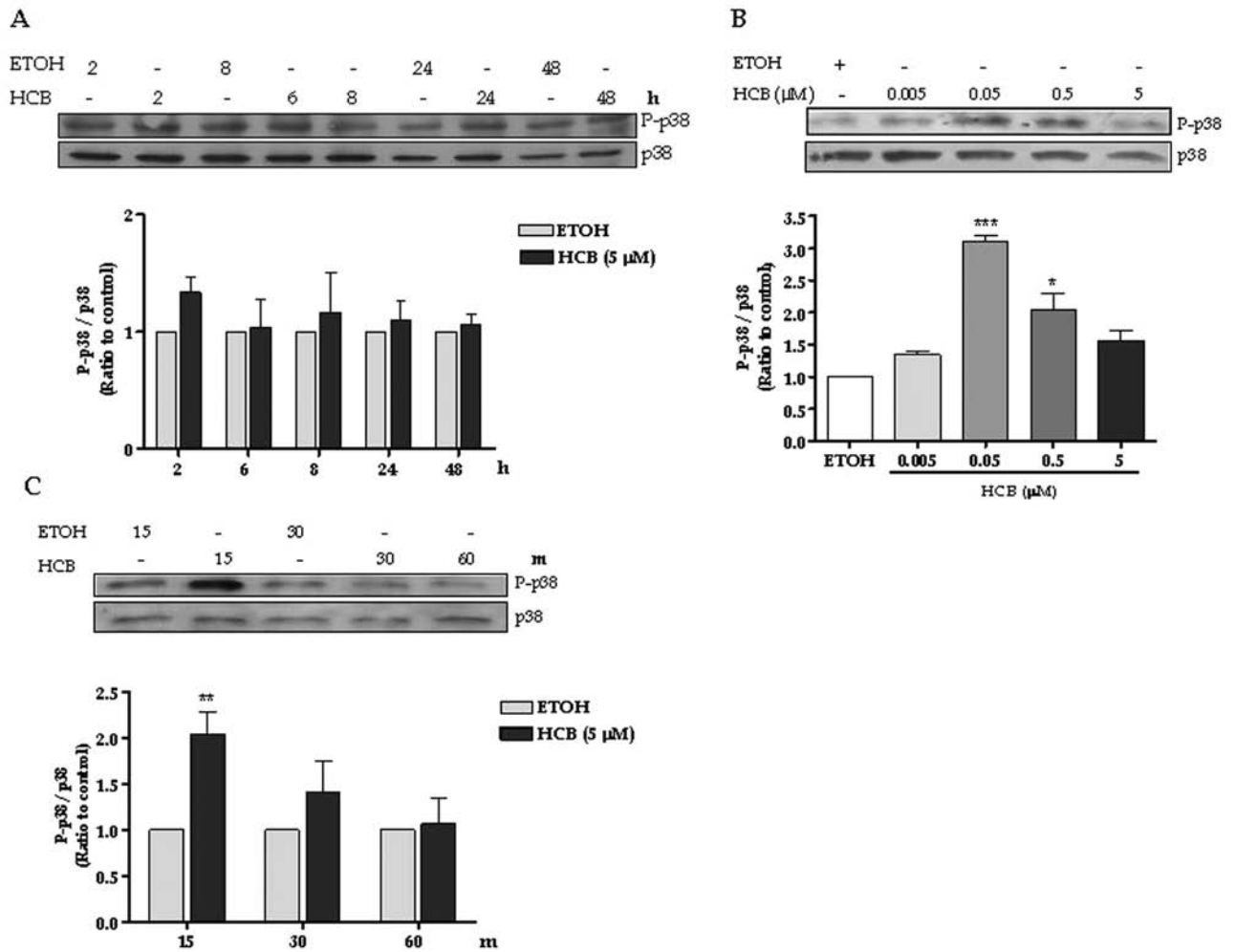
**FIG. 9.** HCB effect on p38 MAPK phosphorylation. Whole-cell lysates were prepared, and proteins were resolved by SDS-PAGE and blotted with the corresponding specific antibodies. Western blots from one representative experiment are shown in the corresponding upper panels. Densitometric scanning of the immunoblots is shown in the lower panels. (A) Time course of p38 MAPK phosphorylation. Quantification of P-p38/p38 ratio to control, (B) dose-response effect of HCB on p38 MAPK phosphorylation. Quantification of P-p38/p38 ratio to control. (C) Transient HCB effect on p38 MAPK phosphorylation. Data are expressed as means ± SEM of three independent experiments. Asterisks indicate significant differences versus ETOH-treated cells. (*$p < 0.05$, **$p < 0.01$, ***$p < 0.001$). Statistical comparisons were made by one-way ANOVA with a 95% confidence interval followed by Tukey *post hoc* test to identify significant differences between mean values and indicated controls.

fission and fusion also actively participate in apoptosis induction (Suen *et al*., 2008). In this study, we have demonstrated that this network disintegrates during HCB-induced apoptosis, yielding more numerous and smaller mitochondria, which have been associated with a collapse of mitochondrial membrane potential (Δψm) (Pendergrass *et al*., 2004). Increased permeability of the outer mitochondrial membrane is associated with disturbances in intracellular ATP synthesis, generation of ROS, release of cytochrome *c* and AIF, and degradation of caspase-3 (Kroemer *et al*., 2007). The other way around, generation of ROS can cause the loss of Δψm and induce apoptosis by releasing proapoptotic proteins such as AIF and cytochrome *c* from mitochondria to the cytosol (Ott *et al*., 2007). In this respect, we have previously reported that HCB-induced apoptosis in rat

thyroid was associated with increases in cytochrome *c* release and procaspase-9 processing to its active product (Chiappini *et al*., 2009). Herein, we observed that the pesticide elicits a massive cytochrome *c* release from mitochondria to cytosol, followed by a rapid decline to basal levels, suggesting that release of cytochrome *c* may play a role in mediating HCB-induced cell death. In agreement, Bobba *et al.* (1999) reported that cytochrome *c* release is an event that occurs early in the commitment phase of the apoptotic process, and that after accumulation, this protein might be progressively degraded by induced caspases. Similarly, AIF release, and its nuclear translocation, which is associated with chromatin condensation and DNA cleavage, was also demonstrated in this study. As both cytosolic and nuclear AIF protein levels are increased
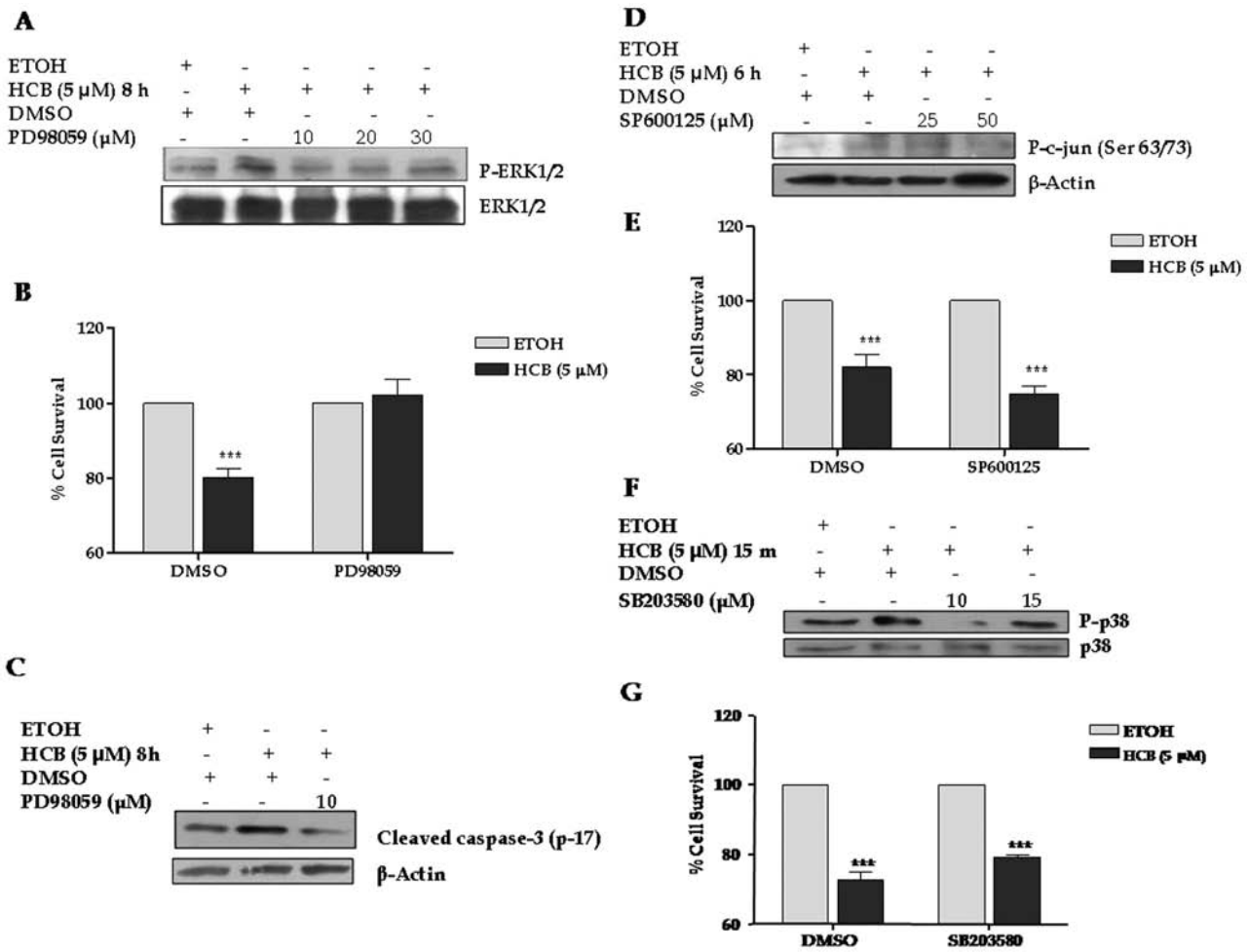
**A**

| ETOH | + | − | − | − | − |
| HCB (5 µM) 8 h | − | + | + | + | + |
| DMSO | + | + | − | − | − |
| PD98059 (µM) | − | − | 10 | 20 | 30 |

P-ERK1/2
ERK1/2

**B**

% Cell Survival

ETOH / HCB (5 µM)
DMSO        PD98059

**C**

| ETOH | + | − | − |
| HCB (5 µM) 8 h | − | + | + |
| DMSO | + | + | − |
| PD98059 (µM) | − | − | 10 |

Cleaved caspase-3 (p-17)
β-Actin

**D**

| ETOH | + | − | − | − |
| HCB (5 µM) 6 h | − | + | + | + |
| DMSO | + | + | − | − |
| SP600125 (µM) | − | − | 25 | 50 |

P-c-jun (Ser 63/73)
β-Actin

**E**

% Cell Survival

ETOH / HCB (5 µM)
DMSO        SP600125

**F**

| ETOH | + | − | − | − |
| HCB (5 µM) 15 m | − | + | + | + |
| DMSO | + | + | − | − |
| SB203580 (µM) | − | − | 10 | 15 |

P-p38
p38

**G**

% Cell Survival

ETOH / HCB (5 µM)
DMSO        SB203580

**FIG. 10.** Roles of ERK1/2, JNK1, and p38 kinase on cell viability. (A) Protein levels of P-ERK1/2 and total ERK1/2 were determined in the total cell lysate pretreated with PD98059. (B) Role of ERK1/2 on cell viability. FRTL-5 cells were pretreated with PD98059 or DMSO and further treated with 5 µM HCB for 24 h in the presence of the inhibitor. Cell viability was evaluated by the MTT assay. (C) Immunodetection of active caspase-3 in total cell lysate, of FRTL-5 cells, pretreated with 10 µM PD98059 or dimethyl sulfoxide (DMSO) and further treated with 5 µM HCB or ETOH for 8 h in the presence of the inhibitor. (D) Effect of JNK1 inhibitor, SP600125, on P-c-jun and β-actin, protein levels, in the total cell lysate, determined by Western blotting. (E) Role of JNK1 on cell survival. FRTL-5 cells were pretreated with SP600125 or DMSO and further treated with HCB or ETOH in the presence of the inhibitor. Cell viability was evaluated by the MTT assay. (F) Effect of p38 MAPK inhibitor, SB203580, on P-p38 and p38 protein levels, determined in the total cell lysate by Western blotting. (G) Role of p38 kinase on cell survival. FRTL-5 cells were pretreated with SB203580 or DMSO, followed by HCB or ETOH exposure. Cell viability was evaluated by the MTT assay. (B, E, and G) Data are expressed as means ± SEM of three independent experiments. Asterisks indicate significant differences versus ETOH-treated cells (***$p < 0.001$). Statistical comparisons were made by two-way ANOVA with a 95% confidence interval followed by Bonferroni's *post hoc* test to identify significant differences between mean values and indicated controls.

with HCB treatment, the possibility exists that the antioxidant decreases AIF release from the mitochondria as well. Numerous *in vitro* and *in vivo* studies have documented antioxidant inhibition of AIF-mediated cell death, supporting the notion that the intracellular ROS level positively regulates AIF cleavage and release from the mitochondria. This event has been associated with the caspase-independent apoptotic pathway (Norberg *et al.*, 2010). Thus, our results show that caspase-dependent and -independent apoptotic signaling pathways are activated in HCB-induced apoptosis in FRTL-5 cells.

An *in vivo* oxidative stress condition in liver from HCB-treated rats has been reported by Ezendam *et al.* (2004). In this study, we

showed for the first time that doses of HCB (0.5 and 5 µM) associated with the increase of parameters of apoptosis induced ROS generation. A close correlation between oxidative stress and degree of apoptosis was also demonstrated in endosulfan-treated human peripheral blood mononuclear cells (Ahmed *et al.*, 2008).

Herein, we have demonstrated that blocking of ROS production with a scavenger such as Trolox resulted in inhibition of AIF nuclear translocation and returned cell survival to control levels, demonstrating that ROS are critical mediators of HCB-induced apoptosis.

ROS generation has been described to activate all MAPK cascades in response to oxidant injury, and they can therefore
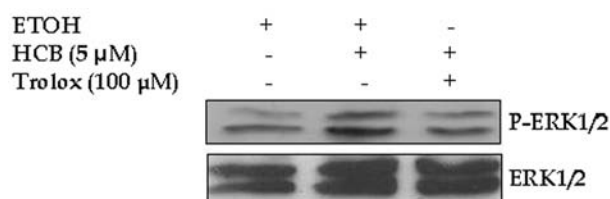
**FIG. 11.** ROS mediate HCB-induced ERK1/2 activation. Immunodetection by Western blot of P-ERK1/2 and total ERK1/2 in the nuclear fraction of FRTL-5 cells pretreated with Trolox and treated with HCB or ETOH in the presence of the antioxidant.

have an impact on cell survival and cell death (Cagnol and Chambard, 2010). Although ERK1/2 is known to be involved in cell survival, evidences suggest that their activation also contributes to cell death in some cell types and organs under certain conditions. In this report, we have demonstrated that ERK1/2, JNK1, and p38 MAPK phosphorylation are stimulated by HCB, following different time-course and dose-response profiles. The complexities of the physiological roles of MAPK may be due partially to the duration of MAPK activities differentially regulating genes in various cell types. Activation of ERK1/2 by organochlorine pesticides has been reported in human keratinocytes (Ledirac et al., 2005). It has been suggested that in situations where ERK1/2 induces cell death, the activation tends to be sustained (Wang et al., 2000), which is the case under our experimental conditions. Conversely, a transient activation of p38 MAPK was observed within 15 min of 5μM HCB treatment, an event that has been related to cell differentiation rather than apoptosis (Nagata and Todokoro, 1999).

Our work demonstrates that ERK1/2 is a critical mediator in HCB-induced loss of cell viability. This statement is based on the observation that when FRTL-5 cells were treated with specific MAPK inhibitors, in the presence of HCB, cell survival was restored to control levels, only when ERK1/2 transduction pathway was inhibited.

On the other hand, we have shown that HCB-induced JNK activation is not involved in loss of cell viability. In this respect, Shklyaev et al. (2001) have demonstrated that epidermal growth factor, transforming growth factor-beta (TGF-beta), and hepatocyte growth factor induced JNK activation but did not trigger apoptotic cell death of human thyrocytes. The authors suggest that JNK activation does not induce apoptosis but is associated with survival or transformation of human thyroid cells.

The mechanism by which ERK1/2 mediates apoptosis has not been well defined. Nowak (2002) reported that ERK1/2 inhibition blocked caspase-3 activation without affecting cytochrome c release from mitochondria. On the other hand, Kaushal et al. (2004) reported that ERK1/2 activation results in depolarization of mitochondrial potential and cytochrome c release, which are generally considered to be a prerequisite for activation of caspase-3. Our study demonstrating that ERK1/2 inhibition blocks HCB-induced activation of caspase-3 do not reveal if ERK1/2 acts downstream of cytochrome c release

or upstream of mitochondria, inducing cytochrome c release. Other authors have reported that ERK1/2 may regulate apoptosis via direct phosphorylation of p53 (Persons et al., 2000), promoting the proapoptotic activities of Bak (Mihara et al., 2003), or through suppression of survival signaling pathways such as the phosphatidylinositol 3-kinase/Akt pathway (Amaravadi and Thompson, 2005). Further studies are needed to define the target(s) where ERK1/2 is coupled to the apoptotic pathway.

Our results revealed that ROS generation is likely the more upstream signal given the ability of Trolox to ablate ERK1/2 activation. A critical role of ROS in organochlorine pesticide-induced ERK1/2 activation, probably by stabilizing its phosphorylation, has been reported (Ledirac et al., 2005). It has been proposed that transient activation of ROS inactivates MAPK regulatory phosphatases, contributing to their activation (Lee and Esselman, 2002).

In conclusion, this study reports for the first time that HCB induces apoptosis in FRTL-5 cells, by ROS-mediated ERK1/2 activation, through caspase-dependent and -independent pathways. Taken together, our results provide a clue to the molecular events involved in the mechanism of action of HCB-induced apoptosis in FRTL-5 thyroid cells.

## SUPPLEMENTARY DATA

Supplementary data are available online at http://toxsci.oxfordjournals.org/.

## FUNDING

## ACKNOWLEDGMENTS

## REFERENCES

Ahmed, T., Tripathi, A. K., Ahmed, R. S., Das, S., Suke, S. G., Pathak, R., Chakraboti, A., and Banerjee, B. D. (2008). Endosulfan-induced apoptosis and glutathione depletion in human peripheral blood mononuclear cells: Attenuation by N-acetylcysteine. J. Biochem. Mol. Toxicol. 22, 299–304.

Almeida, M. G., Fanini, F., Davino, S. C., Aznar, A. E., Koch, O. R., and Barros, S. B. (1997). Pro- and anti-oxidant parameters in rat liver after short-term exposure to hexachlorobenzene. Hum. Exp. Toxicol. 16, 257–261.

Amaravadi, R., and Thompson, C. B. (2005). The survival kinases Akt and Pim as potential pharmacological targets. J. Clin. Invest. 115, 2618–2624.

ATSDR. (2002). Toxicological Profile for Hexachlorobenzene. US Department of Health and Human Services, Washington, DC.

Bobba, A., Atlante, A., Giannattasio, S., Sgaramella, G., Calissano, P., and Marra, E. (1999). Early release and subsequent caspase-mediated

degradation of cytochrome c in apoptotic cerebellar granule cells. *FEBS Lett.* **457,** 126–130.

Bradford, M. M. (1976). A rapid and sensitive method for the quantitation of microgram quantities of protein utilizing the principle of protein-dye binding. *Anal. Biochem.* **72,** 248–254.

Cagnol, S., and Chambard, J. C. (2010). ERK and cell death: Mechanisms of ERK-induced cell death–apoptosis, autophagy and senescence. *FEBS J.* **277,** 2–21.

Chiappini, F., Alvarez, L., Lux-Lantos, V., Randi, A. S., and Kleiman de Pisarev, D. L. (2009). Hexachlorobenzene triggers apoptosis in rat thyroid follicular cells. *Toxicol. Sci.* **108,** 301–310.

Chuang, S. M., Wang, I. C., and Yang, J. L. (2000). Roles of JNK, p38 and ERK mitogen-activated protein kinases in the growth inhibition and apoptosis induced by cadmium. *Carcinogenesis* **21,** 1423–1432.

Ezendam, J., Staedtler, F., Pennings, J., Vandebriel, R. J., Pieters, R., Harleman, J. H., and Vos, J. G. (2004). Toxicogenomics of subchronic hexachlorobenzene exposure in Brown Norway rats. *Environ. Health Perspect.* **112,** 782–791.

Filomenko, R., Prévotat, L., Rébé, C., Cortier, M., Jeannin, J. F., Solary, E., and Bettaieb, A. (2006). Caspase-10 involvement in cytotoxic drug-induced apoptosis of tumor cells. *Oncogene* **25,** 7635–7645.

Frasch, S. C., Nick, J. A., Fadok, V. A., Bratton, D. L., Worthen, G. S., and Henson, P. M. (1998). p38 mitogen-activated protein kinase-dependent and -independent intracellular signal transduction pathways leading to apoptosis in human neutrophils. *J. Biol. Chem.* **273,** 8389–8397.

Giribaldi, L., Chiappini, F., Pontillo, C., Randi, A. S., Kleiman de Pisarev, D. L., and Alvarez, L. (2011). Hexachlorobenzene induces deregulation of cellular growth in rat liver. *Toxicology* **289,** 19–27.

Green, D. R., and Reed, J. C. (1998). Mitochondria and apoptosis. *Science* **281,** 1309–1312.

Grimalt, J. O., Sunyer, J., Moreno, V., Amaral, O. C., Sala, M., Rosell, A., Anto, J. M., and Albaiges, J. (1994). Risk excess of soft-tissue sarcoma and thyroid cancer in a community exposed to airborne organochlorinated compound mixtures with a high hexachlorobenzene content. *Int. J. Cancer* **56,** 200–203.

Guicciardi, M. E., and Gores, G. J. (2005). Apoptosis: A mechanism of acute and chronic liver injury. *Gut* **54,** 1024–1033.

Kalli, K. R., Devine, K. E., Cabot, M. C., Arnt, C. R., Heldebrant, M. P., Svingen, P. A., Erlichman, C., Hartmann, L. C., Conover, C. A., and Kaufmann, S. H. (2003). Heterogeneous role of caspase-8 in fenretinide-induced apoptosis in epithelial ovarian carcinoma cell lines. *Mol. Pharmacol.* **64,** 1434–1443.

Kaushal, G. P., Liu, L., Kaushal, V., Hong, X., Melnyk, O., Seth, R., Safirstein, R., and Shah, S. V. (2004). Regulation of caspase-3 and -9 activation in oxidant stress to RTE by forkhead transcription factors, Bcl-2 proteins, and MAP kinases. *Am. J. Physiol. Renal Physiol.* **287,** F1258–F1268.

Kroemer, G., Galluzzi, L., and Brenner, C. (2007). Mitochondrial membrane permeabilization in cell death. *Physiol. Rev.* **87,** 99–163.

Ledirac, N., Antherieu, S., d'Uby, A. D., Caron, J. C., and Rahmani, R. (2005). Effects of organochlorine insecticides on MAP kinase pathways in human HaCaT keratinocytes: Key role of reactive oxygen species. *Toxicol. Sci.* **86,** 444–452.

Lee, K., and Esselman, W. J. (2002). Inhibition of PTPs by H(2)O(2) regulates the activation of distinct MAPK pathways. *Free Radic. Biol. Med.* **33,** 1121–1132.

Meeker, J. D., Altshul, L., and Hauser, R. (2007). Serum PCBs, p,p'-DDE and HCB predict thyroid hormone levels in men. *Environ. Res.* **104,** 296–304.

Mihara, M., Erster, S., Zaika, A., Petrenko, O., Chittenden, T., Pancoska, P., and Moll, U. M. (2003). p53 has a direct apoptogenic role at the mitochondria. *Mol. Cell* **11,** 577–590.

Nagata, Y., and Todokoro, K. (1999). Requirement of activation of JNK and p38 for environmental stress-induced erythroid differentiation and apoptosis and of inhibition of ERK for apoptosis. *Blood* **94,** 853–863.

Norberg, E., Orrenius, S., and Zhivotovsky, B. (2010). Mitochondrial regulation of cell death: Processing of apoptosis-inducing factor (AIF). *Biochem. Biophys. Res. Commun.* **396,** 95–100.

Nowak, G. (2002). Protein kinase C-alpha and ERK1/2 mediate mitochondrial dysfunction, decreases in active Na+ transport, and cisplatin-induced apoptosis in renal cells. *J. Biol. Chem.* **277,** 43377–43388.

Ott, M., Gogvadze, V., Orrenius, S., and Zhivotovsky, B. (2007). Mitochondria, oxidative stress and cell death. *Apoptosis* **12,** 913–922.

Pendergrass, W., Wolf, N., and Poot, M. (2004). Efficacy of MitoTracker Green and CMXrosamine to measure changes in mitochondrial membrane potentials in living cells and tissues. *Cytometry. A* **61,** 162–169.

Persons, D. L., Yazlovitskaya, E. M., and Pelling, J. C. (2000). Effect of extracellular signal regulated kinase on p53 accumulation in response to cisplatin. *J. Biol. Chem.* **275,** 35778–35785.

Shklyaev, S. S., Namba, H., Mitsutake, N., Alipov, G., Nagayama, Y., Maeda, S., Ohtsuru, A., Tsubouchi, H., and Yamashita, S. (2001). Transient activation of c-Jun NH2-terminal kinase by growth factors influences survival but not apoptosis of human thyrocytes. *Thyroid* **11,** 629–636.

Suen, D. F., Norris, K. L., and Youle, R. J. (2008). Mitochondrial dynamics and apoptosis. *Genes Dev.* **22,** 1577–1590.

To-Figueras, J., Sala, M., Otero, R., Barrot, C., Santiago-Silva, M., Rodamilans, M., Herrero, C., Grimalt, J., and Sunyer, J. (1997). Metabolism of hexachlorobenzene in humans: Association between serum levels and urinary metabolites in a highly exposed population. *Environ. Health Perspect.* **105,** 78–83.

Tsatsoulis, A. (2002). The role of apoptosis in thyroid disease. *Minerva Med.* **93,** 169–180.

Wang, X., Martindale, J. L., and Holbrook, N. J. (2000). Requirement for ERK activation in cisplatin-induced apoptosis. *J. Biol. Chem.* **275,** 39435–39443.

Xia, Z., Dickens, M., Raingeaud, J., Davis, R. J., and Greenberg, M. E. (1995). Opposing effects of ERK and JNK-p38 MAP kinases on apoptosis. *Science* **270,** 1326–1331.